A Theoretical Insight into the Reaction Mechanism of Photochemical Transposition from Pyrazole to Imidazole

Ming-Der Su*

Department of Applied Chemistry, National Chiayi University, Chiayi 60004, Taiwan

Received: June 19, 2008; Revised Manuscript Received: August 06, 2008

The mechanisms of the photochemical isomerization reactions were investigated by using a model system of 1,3,5-trimethylpyrazole (**1**) with the CASSCF (eight-electron/six-orbital active space) and MP2-CAS methods and the 6-311G(d) basis set. Three reaction pathways were examined in the present work. They are denoted as the ring-contraction−ring-expansion path (path I), the internal-cyclization−isomerization path (path II), and the conical-intersection path (path III). Our model investigations suggest that the preferred reaction route for the pyrazoles is as follows: reactant → Franck−Condon region → conical intersection → photoproduct. In particular, the conical-intersection mechanism (path III) found in this work gives a better explanation than the previously proposed two other mechanisms (paths I and II). The theoretical findings also indicate that path III-1 should be favored over path III-2 from a kinetic point of view. This suggests that the quantum yield of 1,2,4-trimethylimidazole (**2**) should be greater than that of 1,2,5-trimethylimidazole (**3**), which supports the available experimental observations. Additionally, we propose a simple p-π orbital topology model, which can be used as a diagnostic tool to predict the location of the conical intersections, as well as the geometries of the phototransposition products of various heterocycles.

I. Introduction

The photochemical behavior of five-membered aromatic compounds containing two heteroatoms has been described for a variety of systems.[1] A general rearrangement process involving the formal interchange of two adjacent atoms has been found to occur as shown in Scheme 1. For different five-membered aromatic heterocycles, these reactions differ in photoproducts and yields. Such photochemical transposition reactions are assumed to proceed via different mechanisms depending on the heteroatom in the ring.[2] Many experiments and theoretical investigations have been carried out to derive the mechanisms involved.[1,2]

As pointed out by Padwa,[2] a great deal of experimental work has been done on the photochemical rearrangement reactions of pyrazoles to imidazoles.[3−5] For instance (see Scheme 2), Schmid and co-workers reported that 1-methylpyrazole undergoes photoisomerization to 1-methyl imidazole as given in eq 1.[3f] Beak and co-workers observed that 1,3,5-trimethylpyrazole phototransposes to 1,2,4-trimethylpyrazole and 1,2,5-trimethylpyrazole, as demonstrated in eq 2.[3e,k] Interested readers can find excellent articles in refs 4 and 5. Essentially, two mechanisms, that is, ring contraction−ring expansion (see Scheme 3) and internal cyclization−isomerization[2] (see Scheme 4), have been proposed to explain and rationalize such phototranspositions. To the best of our knowledge, only the parent pyrazole species has been the subject of previous theoretical treatment based on the MNDO method performed by Connors, Pavlik, and co-workers.[5b] However, their published work concerning the photoisomerization of pyrazole posed a number of unsolved mechanistic and logical questions, because they used a semiempirical method which is well-known to be unreliable for explaining many photochemical reactions.[6] Besides this, to the best of our knowledge, there has been so far no attempt to arrive at the photochemical transposition reactions of pyrazoles.

SCHEME 1

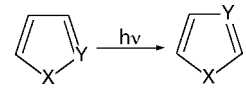

SCHEME 2

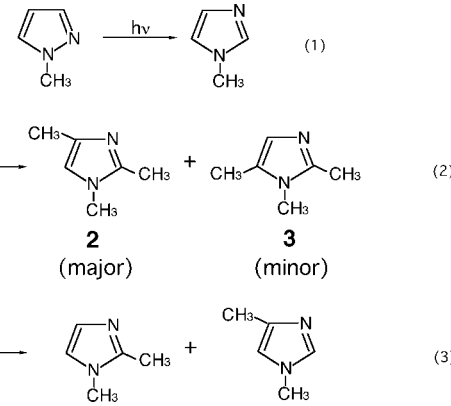

SCHEME 3

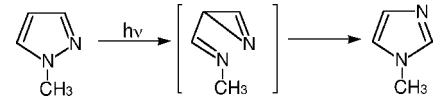

In such a case, theoretical information is of great help for further advance in pyrazole photochemistry. In fact, a detailed understanding of the photochemistry of pyrazoles is of interest not only for the advancement of basic science but also for the continued development of its applications. We have thus undertaken ab initio calculations of the reaction mechanisms of the phototransposition of pyrazole to imidazole in order to

* Corresponding author. E-mail: midesu@mail.ncyu.edu.tw.

10.1021/jp805394k CCC: $40.75
Published on Web 09/18/2008

SCHEME 4

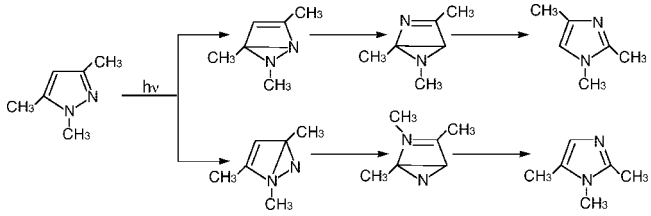

extend our knowledge of pyrazole photobehavior. In this work, one phototransposition reaction (i.e., eq 2) was used to examine mechanistic details by using CASSCF and CASMP2 theories. The pyrazole species used is 1,3,5-trimethylpyrazole (**1**). There are three reasons for selecting this trisubstituted system. First, the theoretical results obtained from the present study can be compared with the available experimental observations. Second, it is intriguing because of the high selecivity of bond breaking that demands an explanation. And third, it is also intriguing because it offers the possibility of distinction between reactant and product.

As mentioned earlier, two basic reaction mechanisms have been used traditionally to rationalize such *N*-methylpyrazole → *N*-methylimidazole phototransposition reactions.[2−5] However, recently, it has been shown clearly that the stereochemical outcome of the photoreactions cannot be interpreted in terms of bicyclic minima and excimer minima and the barriers between them. Instead, the main feature of many photoreactions is the existence of a real conical intersection (CI).[6] That is to say, most photochemical reactions of molecules start on an excited electronic potential surface but cross over to a lower potential energy surface somewhere along the reaction pathway. They finally reach the ground-state surface by a sequence of radiationless transitions (i.e., CIs) and move on the ground-state surface toward the product.[6] This mechanism is not controlled by the avoided surface crossing and the resulting energy gap between ground and excited state but rather by the presence of minima and transition states on ground- and excited-state surfaces themselves. Furthermore, the existence of a CI region provides access to a number of ground-state pathways that can lead to different photoproducts.[7] This has already been both experimentally and theoretically proved to be a general feature of the excited states relevant to photochemical reactions.[6,7]

Our approach is to calculate a number of mechanisms of the phototranspositions of pyrazoles for which activation parameters are available. Even if the uncertainties in the calculated activation parameters for individual reactions are too large for definite conclusions to be drawn from them, the relative values for a number of related reactions are likely to be reproduced, at least qualitatively. Comparison of the predicted pattern of rates with experiments should then provide a more reliable test of the predicted mechanisms than any calculation for a single case. It will be shown below that the CI[6,7] plays a crucial role in the photoisomerization of these aromatic pyrazole systems.

II. Methodology

All the geometries were fully optimized without imposing any symmetry constraints, although in some instances, the resulting structures showed various elements of symmetry. The ab initio molecular orbital calculations were performed by using the Gaussian 03 software package.[8]

Recent ab initio CASSCF (the complete-active-space SCF) investigations of the potential energy surfaces of the ground and excited states of polyatomic molecules have indicated that low-lying CIs occur with previously unsuspected frequency.[6,7] The geometry optimizations were carried out by using the CASSCF method combined with the 6-311G(d) basis set. Eight electrons in the five p-π and one nonbonding orbitals were included in the active space (vide infra). The state-averaged CASSCF(8,6) method was used to determine geometry on the intersection space. The optimization of CIs was achieved in the $(f - 2)$-dimensional intersection space using the method of Bearpark et al.[9] implemented in the Gaussian 03 program. Every stationary point was characterized by its harmonic frequencies computed analytically at the CASSCF level. Localization of the minima and CI minima were performed in Cartesian coordinates; therefore, the results are independent of any specific choice of internal variables.

To correct the energetics for dynamic electron correlation, we have used the multireference Møller−Plesset (MP2-CAS) algorithm[10] as implemented in the program package GAUSSIAN 03. Unless otherwise noted, the relative energies given in the text are those determined at the MP2-CAS-(8,6)/6-311G(d) level by using the CAS(8,6)/6-311G(d) (hereafter designed MP2-CAS and CASSCF, respectively) geometry.

III. General Considerations

It was reported that the experimental absorption spectra of unsubstituted pyrazole in various solvent exhibit two broad bands with maxima (λ_{max}) between 206 and 210 nm (= 139 and 136 kcal/mol) depending on the solvent.[11] They are experimentally assigned to the singlet $^1\pi \rightarrow {}^1\pi^*$ transition.[11] To the author's knowledge, there has been no report of the gas-phase UV spectrum of pyrazole. That is to say, all experimental information on the electronic spectrum of unsubstituted pyrazole stems from measurements in liquids. Moreover, experimental geometries and spectra for the 1,3,5-trimethylpyrazole (**1**) species studied in the present work are not available to allow a definitive comparison. Nevertheless, experimentalists have found no indication of the participation of a triplet state in the photoisomerization of this species.[4,5] Namely, the triplet state plays no role in the photoreactions studied in the present work. In consequence, the photoisomerization reactions of the methyl-substituted pyrazole should proceed on singlet surfaces and only involve the $\pi \rightarrow \pi^*$ transition. We shall therefore focus on $^1(\pi, \pi^*)$ surfaces from now on.

In order to confirm the accuracy of the theoretical calculations presented in this work, we next consider the Franck−Condon (FC) effect, which should play an important role in the photochemical reactions. In the first step, the reactant is excited to its singlet state by a vertical excitation. However, as mentioned above, no experimental results, neither solution nor gas phase, are available for the vertical transition of **1** itself. Nonetheless, our MP2-CAS result estimates that the $^1\pi \rightarrow {}^1\pi^*$ excited-state energy at the FC geometry for trimethylpyrazole (**1**) is 156 kcal/mol (183 nm). This value for **1** agrees reasonably with the experimental observations for unsubstituted pyrazole as stated earlier.[5b,11] When bearing in mind that this model reactant contains three methyl substituents, we feel that the accuracy of the calculations is sufficient for the following investigations of the mechanisms of photorearrangements (vide infra).

A general outline of the five p-π orbitals in unsubstituted pyrazole is shown explicitly in Scheme 5. As can be seen, the lowest singlet $\pi \rightarrow \pi^*$ excitation is the singlet π_3 (HOMO) → π_4^* (LUMO) transition. It is noteworthy that mixing of π and π^* levels in pyrazole redistributes the electron density. In consequence, in the perturbed HOMO level, the electron density

SCHEME 5

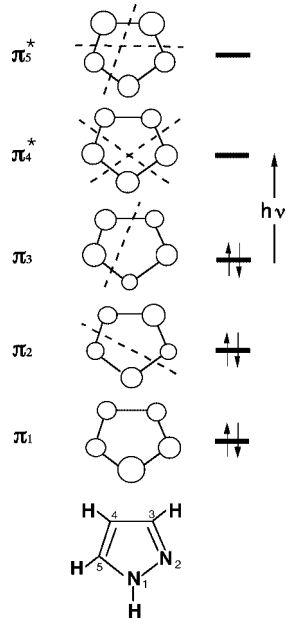

(via the atomic orbital coefficients) is increased on the two ortho-position carbon atoms (C_4 and C_5) with a reduced density on the protonated nitrogen atom (N_1). On the other hand, the coefficients at the protonated nitrogen and the two ortho positions have increased in the perturbed LUMO level. Because the π-electronic structures of methyl-substituted pyrazoles are analogous to those of unsubstituted pyrazole, their photoexcitations should be comparable. In fact, methyl substitution in pyrazole might change the energy of excited states slightly owing to methyl hyperconjugation, but the basic photoexcitation features are not expected to change significantly. Again, it is believed that the present model with the current methods (CASSCF and MP2-CAS) employed in this study should provide reliable information for the discussion of the reaction mechanism.

The central novel feature of the photochemical mechanisms of the methyl-substituted pyrazole (**1**) is the location of its CI in the excited and ground electronic states. In the present work, we shall use the p-π orbital model as outlined in Scheme 5 to search for the CI of photoisomerization of **1**, which is π valence isoelectronic to benzene. Figure 1 shows the qualitative potential energy surfaces for the S_0 and S_1 states of **1** as a function of rotation about the N═C double bond (i.e., the rotation angle θ).[12] By twisting the N═C π bond in **1**, both π_3 and π_4* are raised in energy because of increased antibonding interactions. Consequently, these π orbitals become degenerate at a geometry around 60 and 55° rotation for **1** (path III-1, vide infra) and **1** (path III−2, vide infra), respectively, as shown in Figure 1. In other words, this excitation removes the barrier to rotation about the former N═C axis. Besides, rotation toward an out-of-plane orientation of the p-π orbitals lowers the energy of the excited state. See Scheme 6. Although these out-of-plane angles were obtained without full optimization of the reactant, they at least gave us a hint that a degeneracy between HOMO and LUMO can exist after the rotation of one N═C bond. Moreover, the formation of such a degenerate point provides further evidence for an enhanced intramolecular rotation in the five-membered ring geometry and possibly the existence of a CI, where decay to the ground state can be fully efficient. Accordingly, we shall utilize the above results to interpret the mechanisms for the photochemical isomerization reactions of **1** in the following section.

IV. Results and Discussion

Let us consider the photoisomerization of 1,3,5-trimethylpyrazole (**1**) as indicated in eq 2. As mentioned previously, there are three possible kinds of reaction mechanisms for the pyrazole photorearrangement reactions. That is, the ring-contraction−ring-expansion route (paths I-1 and I-2), the internal-cyclization−isomerization route (paths II-1 and II-2), and the CI route (paths III-1 and III-2), which all lead to the same photoproducts, 1,2,4-trimethylimidazole (**2**) and 1,2,5-trimethylimidazole (**3**), respectively. These reaction routes are all collected in Figures 2, 4, and 6, respectively, which contain the relative energies of the various points with respect to the energy of the reactant 1,3,5-trimethylpyrazole (**1**). These relative energies obtained by using both CASSCF and MP2-CAS methods are presented in Table 1. The structures of the various critical points on the possible mechanistic pathways of Figures 2, 4, and 6 are illustrated in Figures 3, 5, and 7, respectively.

1. Ring-Contraction−Ring-Expansion Mechanism. We first explore the mechanism of path I, the so-called ring-contraction−ring-expansion mechanism. In the first step, the reactant (1,3,5-trimethylpyrazole, **1**) is promoted to its excited singlet state by a vertical excitation as shown in the left-hand of Figure 2. After the vertical excitation process, the molecule is situated on the excited singlet surface but still possesses the S_0 (ground state) geometry (**FC-1**). From the point reached by the vertical excitation, the molecule relaxes to reach an S_1/S_0 CI, where the photoexcited system decays nonradiatively to S_0. Specifically, the photochemically active relaxation path, starting from the S_1 $^1(\pi_3 \rightarrow \pi_4^*)$ excited state of 1,3,5-trimethylpyrazole, leads to either S_1/S_0 **CI−I-1** (path I-1) or **CI−I-2** (path I-2). These paths are shown in the right-hand side of Figure 2.

The geometries at the CIs S_1/S_0 **CI−I-1** and **CI−I-2** are given in Figure 3. Our theoretical findings suggest that S_1/S_0 **CI−I-1** and **CI−I-2** are 41 and 47 kcal/mol lower in energy than **FC-1** at the MP2-CAS level of theory, respectively. The main difference between **1** and S_1/S_0 **CI−I-1** and **CI−I-2** is that the former is a five-membered ring molecule, whereas the latter two are three-membered ring species. In Figure 3, we also give the directions of the derivative coupling and gradient difference vectors for the S_1/S_0 **CI−I-1** and **CI−I-2**. As a result, funneling through the S_1/S_0 **CI−I-1** or **CI−I-2** CIs can each lead to two different reaction pathways on the ground-state surface via either the derivative-coupling vector or the gradient-difference vector direction.[6] Any linear combination of these vectors causes the degeneracy to be lifted, and therefore, these vectors give an indication of possible reaction pathways available on the ground-state surface after decay. In the I-1 pathway, as demonstrated in Figure 3, the major contribution of the gradient-difference vector of S_1/S_0 **CI−I-1** involves three-membered-ring expansion, whereas the derivative-coupling vector corresponds to the concerted CN bond stretching motion. Furthermore, following the gradient difference vector from S_1/S_0 **CI−I-1** leads to the formation of a monocyclic isomer **Min−I-1**. This then undergoes a ring opening via a transition state (**TS−I-1**) to form the final product 1,2,4-trimethylimidazole (**2**). Similarly, in the I-2 pathway, the dominant contribution of the gradient-difference vector of S_1/S_0 **CI−I-2** also involves three-membered-ring expansion, whereas the derivative-coupling vector corresponds to the CN bond stretching motion. Then, following the gradient-difference vector from S_1/S_0 **CI−I-2** can result in the formation of the isomer **Min−I-2**. Again, inspection of the transition vector shows clearly that the reaction proceeds toward formation of the other photoproduct 1,2,5-trimethylimidazole (**3**). That is to

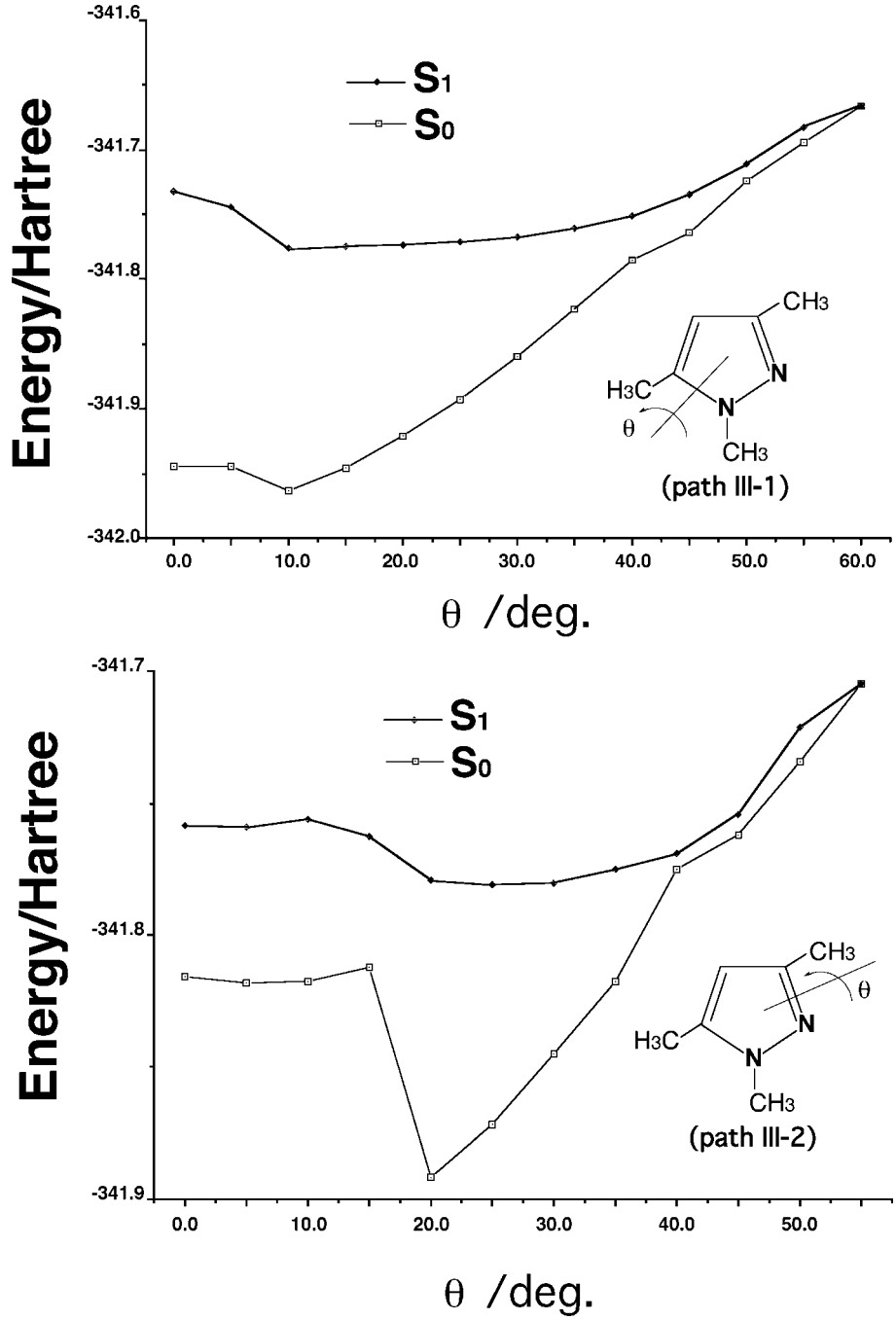

Figure 1. Minimum-energy pathway of 1,3,5-trimethylpyrazole (**1**) along the torsion angle coordinate optimized for the S_1 state at the CAS(8,6)/6-311G(d) level of theory. Two reaction paths of the photoisomerizations of **1** are proposed: path III-1 (top) and path III-2 (bottom).

say, the computational results suggest that the mechanism for paths I-1 and I-2 should proceed as follows:

Path I-1: $\mathbf{1}(S_0) +$

$$h\nu \rightarrow \mathbf{FC-1} \rightarrow \mathbf{CI-I-1} \rightarrow \mathbf{Min-I-1} \rightarrow \mathbf{TS-I-1} \rightarrow \mathbf{2} \quad (1)$$

Path I-2: $\mathbf{1}(S_0) +$

$$h\nu \rightarrow \mathbf{FC-1} \rightarrow \mathbf{CI-I-2} \rightarrow \mathbf{Min-I-2} \rightarrow \mathbf{TS-I-2} \rightarrow \mathbf{3} \quad (2)$$

Besides this, our MP2-CAS results indicate that the relative energetics of these critical points for path I-1 are 156, 115, 74, 127, and −35 kcal/mol for **FC−1**, S_1/S_0 **CI−I-1**, **Min−I-1**, **TS−I-1**, and **2**, respectively, with respect to **1**. On the other hand, the relative energetics of the various points for path I-2 are 156, 109, 19, 70, and −35 kcal/mol for **FC−1**, S_1/S_0 **CI−I-2**, **Min−I-2**, **TS−I-2**, and **3**, respectively, with respect to **1**.

SCHEME 6

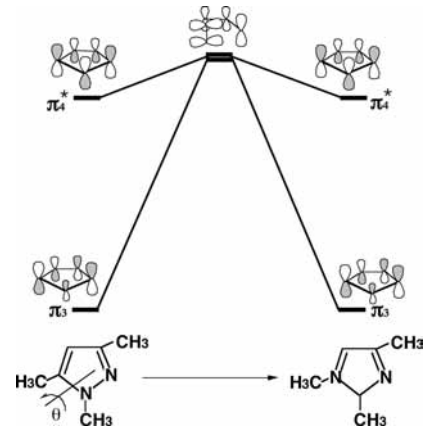

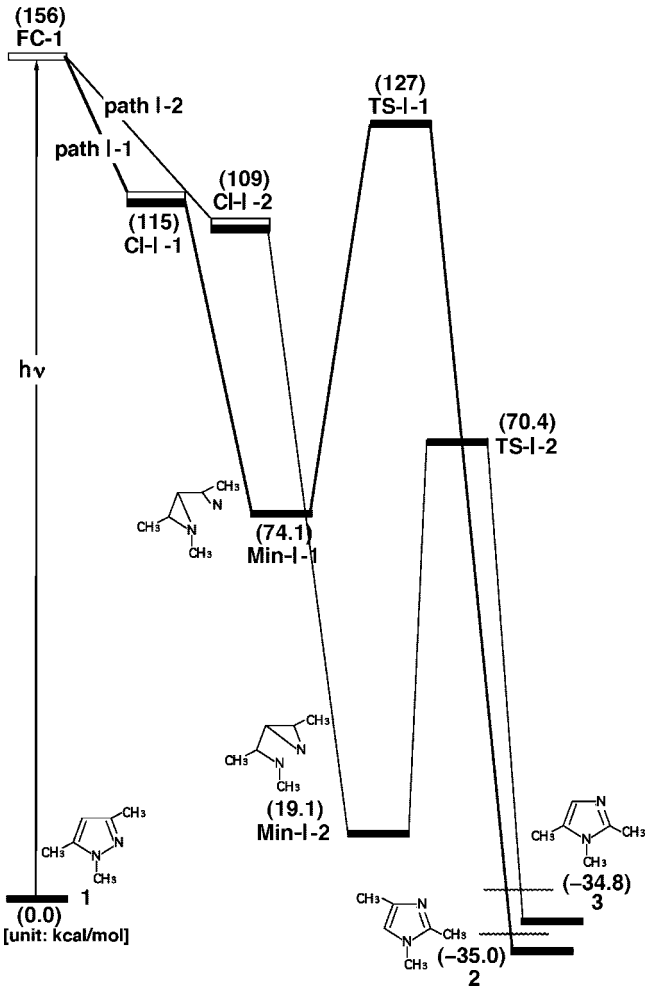

Figure 2. Energy profiles for the photoisomerization modes of 1,3,5-trimethylpyrazole (**1**). The abbreviations FC and CI stand for Frank−Condon and conical intersection, respectively. The relative energies were obtained at the MP2-CAS-(8,6)/6-311G(d)//CAS(8,6)/6-311G(d) level of theory. All energies (in kcal/mol) are given with respect to the reactant (**1**). For the CASSCF optimized structures of the crucial points, see Figure 3. For more information, see the text.

Owing to the high excess energy (82 and 137 kcal/mol) produced from **FC**−**1** to **Min**−**I-1** and **Min**−**I-2**, respectively, it is expected that these relaxation energies are sufficient to provoke the effective photoisomerization reactions (paths I-1, and I-2) for **1**. In particular, when considering the energy barriers for these two reaction paths, our theoretical investigations suggest that the competing photoisomerization of **1** should prefer path I-2, leading to the photoproduct **3**. However, this theoretical result does not agree with the experimental observations.[3] We shall discuss this reaction pathway again in a later section.

2. Internal-Cyclization−Isomerization Mechanism. We next investigate reaction path II, that is, the so-called internal-cyclization−isomerization mechanism. This mechanism is somewhat similar to the mechanism of path I discussed above. From the point (**FC**−**1**) reached by the vertical excitation, the molecule relaxes to reach an S_1/S_0 CI where the photoexcited system decays nonradiatively to S_0. Specifically, the photochemically active relaxation path, starting from the S_1 $^1(\pi_3 \rightarrow \pi_4^*)$ excited state of 1,3,5-trimethylpyrazole (**1**), leads to S_1/S_0 **CI**−**II-1** (path II-1) or **CI**−**II-2** (path II-2). These paths are shown on the right-hand side of Figure 4. All these CI structures optimized at the CASSCF/6-311G(d) level are collected in Figure 5. The derivative-coupling and gradient-difference vectors obtained at these CIs are also represented in Figure 5.

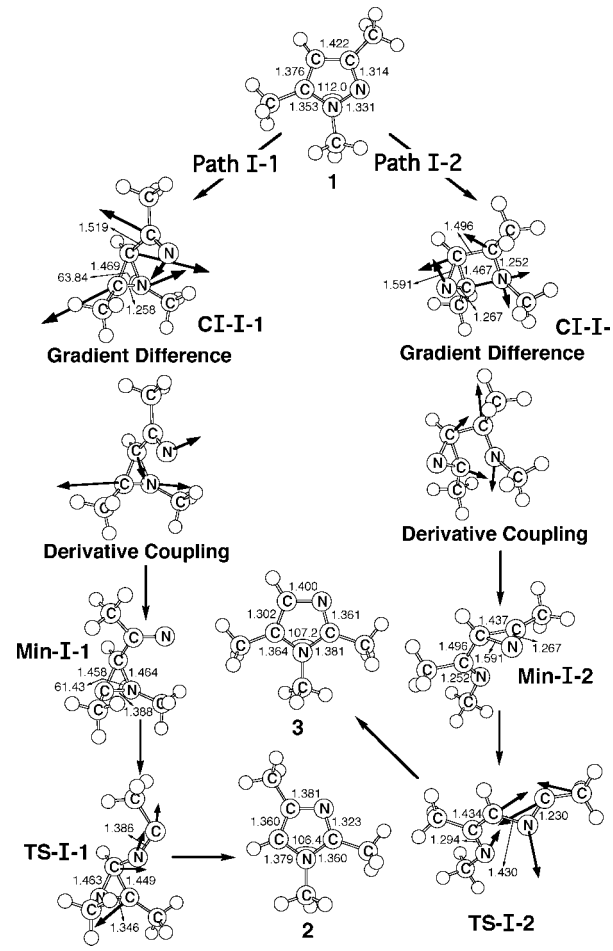

Figure 3. The CAS(8,6)/6-311G(d) geometries (in Å and deg) for path I-1 and path I-2 of 1,3,5-trimethylpyrazole (**1**), CI, intermediate, transition state (TS), and isomer products. The derivative coupling and gradient difference vectors—those which lift the degeneracy—computed with CASSCF at the **CI**−**I-1** and **CI**−**I-2**. The corresponding CASSCF vectors are shown as inset.

We shall first discuss the S_1/S_0 CI **CI**−**II-1**. From the structure of **CI**−**II-1**, the nature of the relaxation path on the S_1 potential surfaces is regarded as N_2-C_5 bond formation. As can be seen in Figure 4, our theoretical findings suggest that the energy of **CI**−**II-1** lies 106 kcal/mol above that of **1** and only 50 kcal/mol lower than that **FC**−**1**. Funneling through the CI, different reaction pathways on the ground-state surface may be predicted by following the derivative coupling vector or the gradient-difference vector direction.[6] As demonstrated in Figure 5, the major contribution of the derivative coupling vector involves the N_2-C_5 bond formation motion, whereas the gradient difference vector corresponds to the N_2-C_3 and C_4-C_5 bond bending motion that leads to a vibrationally hot **1**-S_0 species.

As a consequence, following the derivative coupling vector from S_1/S_0 **CI**−**II-1** (Figure 4) leads to the formation of bicyclic intermediate **Min**−**II-1**. The local minimum **Min**−**II-1** is calculated to be 48 kcal/mol lower than **CI**−**II-1** but is 58 kcal/mol higher than that of the reactant **1**. The next reaction step is a [1,3] sigmatropic shift of the $N-CH_3$ group from N_2 to C_4, which takes place through transition state **TS**−**II-1** in Figure 4. Normal-mode analysis confirms that this structure has one imaginary frequency, $327i$ cm^{-1}, and IRC calculations indicate that **TS**−**II-1** connects **Min**−**II-1** with **Min**−**II-2**. The barrier height at **TS**−**II-1** measured from **Min**−**II-1** is 42 kcal/mol. Once **Min**−**II-2** is formed, the four-membered ring opening

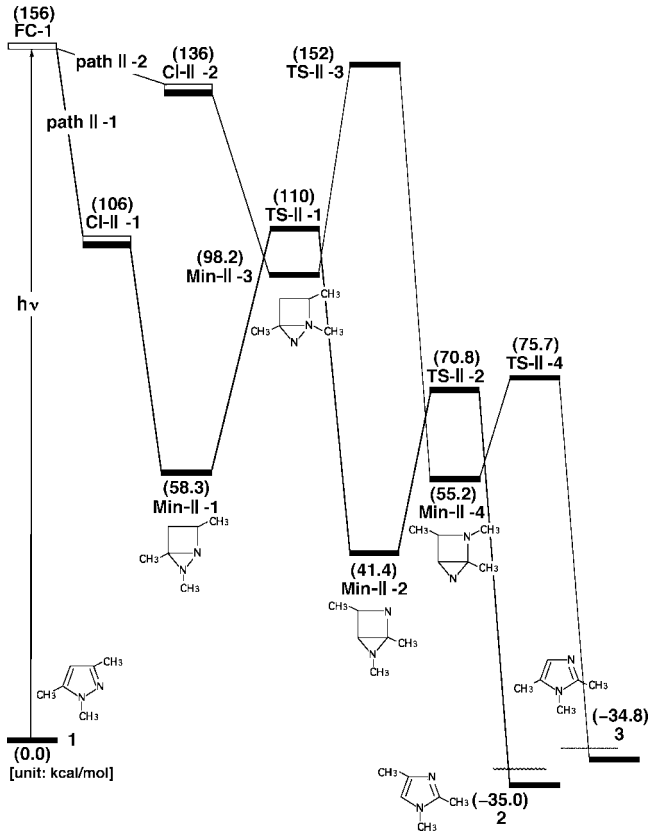

Figure 4. Energy profiles for the photoisomerization modes of 1,3,5-trimethylpyrazole (**1**). The abbreviations FC and CI stand for Frank−Condon and conical intersection, respectively. The relative energies were obtained at the MP2-CAS-(8,6)/6-311G(d)//CAS(8,6)/6-311G(d) level of theory. All energies (in kcal/mol) are given with respect to the reactant (**1**). For the CASSCF optimized structures of the crucial points, see Figure 5. For more information, see the text.

TABLE 1: Energies (in kcal/mol) of the Critical Points Located along the Pathways I-1, I-2, II-1, II-2, III-1, and III-3 at the MP2-CAS-(8,6)/6-311G(d)//CAS(8,6)/6-311G(d) and CAS(8,7)/6-311G(d,p) (in Parentheses) Levels of Theory

structure	state	ΔE rel[a]
1,3,5-trimethylpyrazole (**1**)	S_0	0.0 (0.0)
FC-1	S_1	156.1 (147.5)
CI−I-1	S_1/S_0	115.4 (116.5)
Min-I-1	S_0	74.10 (68.54)
TS-I-1	S_0	127.3 (139.2)
CI−I-2	S_1/S_0	109.0 (114.9)
Min-I-2	S_0	19.13 (6.846)
TS-I-2	S_0	70.39 (75.11)
CI−II-1	S_1/S_0	106.2 (110.0)
Min-II-1	S_0	58.31 (59.96)
TS-II-1	S_0	110.2 (115.3)
Min-II-2	S_0	41.40 (43.46)
TS-II-2	S_0	70.82 (75.17)
CI−II-2	S_1/S_0	136.3 (146.8)
Min-II-3	S_0	98.15 (105.8)
TS-II-3	S_0	152.4 (146.7)
Min-II-4	S_0	55.23 (58.70)
TS-II-4	S_0	75.72 (77.65)
CI−III-1	S_1/S_0	95.26 (100.9)
CI−III-2	S_1/S_0	115.4 (133.0)
1,2,4-trimethylimidazole (**2**)	S_0	−34.99 (104.2)
1,2,5-trimethylimidazole (**3**)	S_0	−34.80 (−1.953)

[a] Energy relative to 1,3,5-trimethylpyrazole (**1**).

by C−C bond activation can take place via the transition state **TS−II-2**, which is 29 kcal/mol above **Min−II-2**. This leads to final photoproduct **2**.

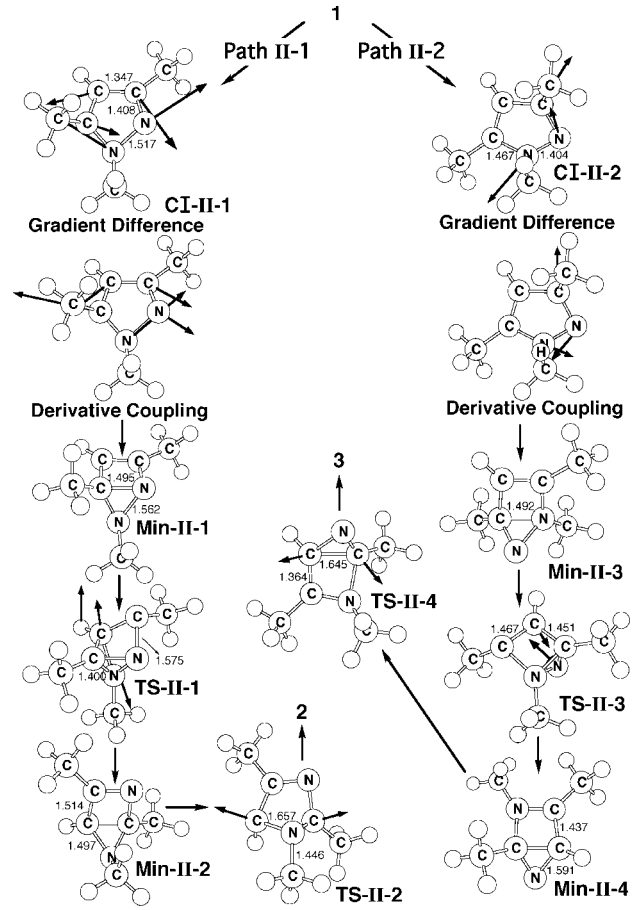

Figure 5. The CAS(8,6)/6-311G(d) geometries (in Å and deg) for path II-1 and path II-2 of 1,3,5-trimethylpyrazole (**1**), CI, intermediate, transition state (TS), and isomer products. The derivative coupling and gradient difference vectors—those which lift the degeneracy—computed with CASSCF at **CI−II-1** and **CI−II-2**. The corresponding CASSCF vectors are shown as inset.

On the other hand, we next investigate the S_1/S_0 **CI−II-2**. The geometrical structure of S_1/S_0 **CI−II-2** can be found in Figure 5, which also contains the derivative coupling and gradient-difference vectors. The geometry of this CI is somewhat similar to the geometry found for S_1/S_0 **CI−II-1** of the 1,3,5-trimethylpyrazole (**1**) system. Following the gradient difference vector from S_1/S_0 **CI−II-2** and decreasing the N_1-C_3 distance, as seen in Figure 5, results in the formation of the bicyclic intermediate **Min−II-3**. Then, the system undergoes a 1,3-sigmatropic shift of the N_2 atom via a transition state **TS−II-3** to give another bicyclic species **Min−II-4**. From there, isomerization can take place with ring opening to produce the 1,2,5-trimethylimidazole (**3**) product (path II-2). As a result, our theoretical investigations suggest that the reaction mechanisms for path II-1 and path II-2 should proceed as follows:

$$\text{Path II-1: } \mathbf{1}(S_0) + h\nu \rightarrow \mathbf{FC-1} \rightarrow \mathbf{CI-II-1} \rightarrow \mathbf{Min-II-1} \rightarrow \mathbf{TS-II-1} \rightarrow \mathbf{Min-II-2} \rightarrow \mathbf{TS-II-2} \rightarrow \mathbf{3} \quad (3)$$

$$\text{Path II-2: } \mathbf{1}(S_0) + h\nu \rightarrow \mathbf{FC-1} \rightarrow \mathbf{CI-II-2} \rightarrow \mathbf{Min-II-3} \rightarrow \mathbf{TS-II-3} \rightarrow \mathbf{Min-II-4} \rightarrow \mathbf{TS-II-4} \rightarrow \mathbf{3} \quad (4)$$

From the two local minima (**Min−II-1** and **Min−II-3**), both isomerizations possess barrier heights computed to be about 52 kcal/mol for **Min−II-1** → **TS−II-1** and 54 kcal/mol for **Min−II-3** → **TS−II-3**. Because of the large excess energy of 156 kcal/mol obtained from the decay of **FC−1** to **1**, both

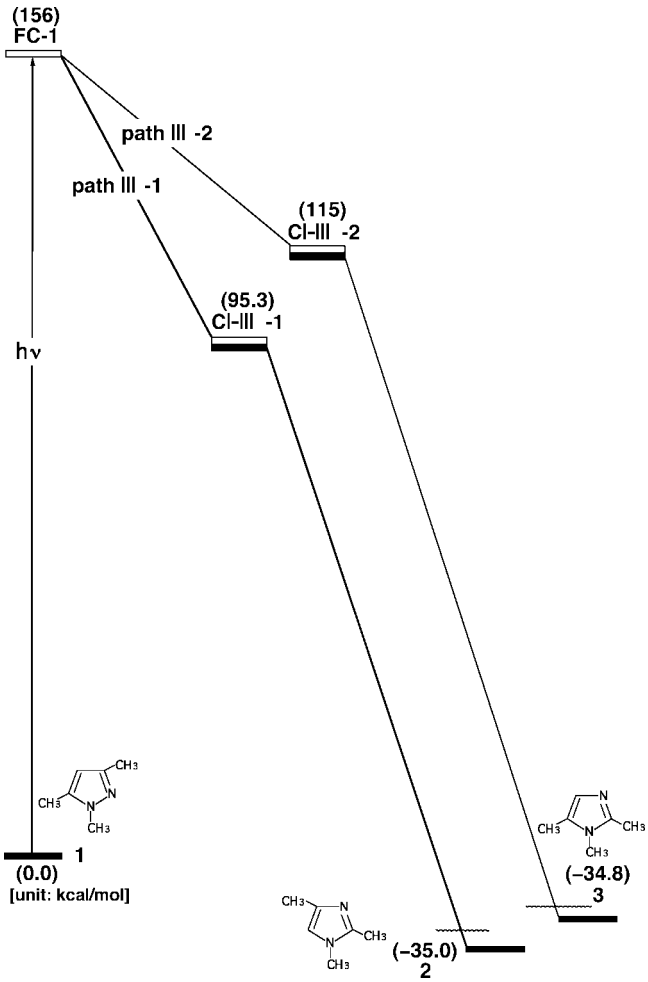

Figure 6. Energy profiles for the photoisomerization modes of 1,3,5-trimethylpyrazole (**1**). The abbreviations FC and CI stand for Frank−Condon and conical intersection, respectively. The relative energies were obtained at the MP2-CAS-(8,6)/6-311G(d)//CAS(8,6)/6-311G(d) level of theory. All energies (in kcal/mol) are given with respect to the reactant (**1**). For the CASSCF optimized structures of the crucial points, see Figure 5. For more information, see the text.

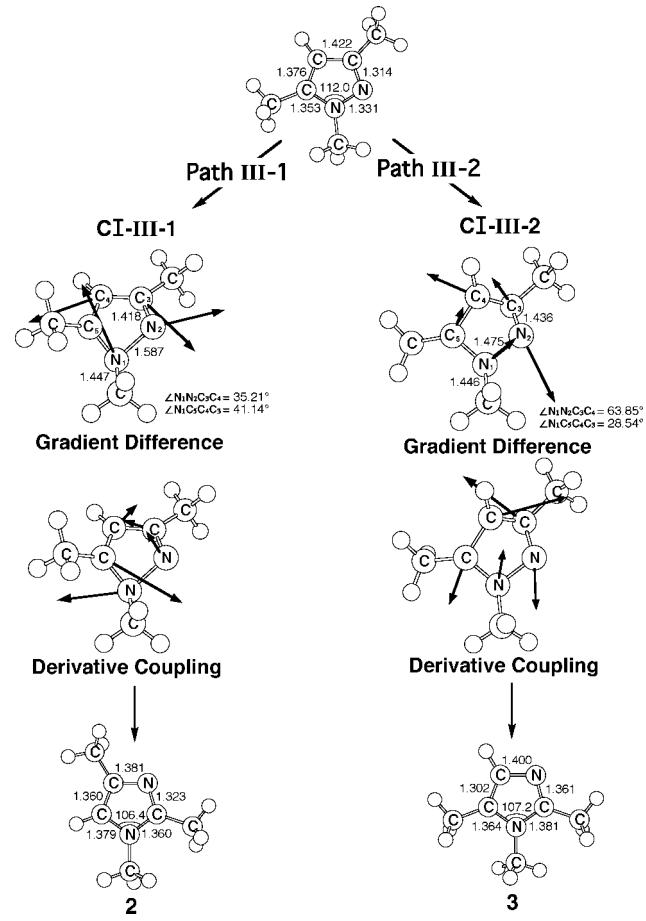

Figure 7. The CAS(8,6)/6-311G(d,p) geometries (in Å and deg) for path III-1 and path III-2 of of 1,3,5-trimethylpyrazole (**1**), CI (**CI**), and isomer product. The derivative coupling and gradient difference vectors—those which lift the degeneracy—computed with CASSCF at **CI−III-1** and **CI−III-2**. The corresponding CASSCF vectors are shown as inset.

barriers can easily be surmounted. Furthermore, the barrier height for path II-1 is slightly lower in energy than that for path II-2 by about 2.0 kcal/mol. Owing to such a small energy difference between two reaction paths, our theoretical findings suggest that path II-1 and path II-2 should compete with each other during the photoreactions of **1**.

3. CI Mechanism. Finally, we explore the mechanism of path III, which only contains one CI point (S_1/S_0 **CI−III-1** and **CI−III-2**) for each reaction pathway (paths III-1 and III-2). The potential-energy profiles for photoisomerization of **1** to produce various imidazoles at the MP2-CAS levels are given in Figure 6. Their selected geometrical parameters are collected in Figure 7, together with the nonadiabatic coupling and gradient-difference vectors of the CI points.

On the basis of the earlier predictions (Figure 1), we searched for a conical crossing point between the S_0 and S_1 surfaces for mechanism III. As shown in Figure 1, because the formation of a narrow energy gap between the S_0 and S_1 states occurs via a twist around one N=C double bond, it implies the existence of a CI in a nearby geometry. Geometry optimization on the S_1 ($\pi_3 \rightarrow \pi_4^*$) excited state is thus performed by twisting structure **1**. The photochemically active relaxation path starting from the S_1 ($\pi_3 \rightarrow \pi_4^*$) excited state of the C_1 structure of **1** leads to the S_1/S_0 CI where the photoexcited system decays nonradiatively to S_0. As a result, the lowest-energy point of the intersection seam of the S_0 and S_1 states was located for each reaction path, and the states are identified as **CI−III-1** and **CI−III-2**, respectively, as presented in Figure 6. As can be seen in Figure 7, the most characteristic feature in the geometries of these CIs is that one C−N bond lies out of the molecular plane as predicted earlier. Namely, in forming the CI structures, planarity is lost, and one N atom moves out of plane by 67° (**CI−III-1**) and 64° (**CI−III-2**). Accordingly, from the structures at these S_1/S_0 CI points, the nature of the relaxation path on the S_1 potential surface can be regarded as C−C and N-N bond cleavage leading to the exchange of two neighboring atoms. These calculations suggest that the geometry of the CI, from which it undergoes intramolecular rotation, is close to the geometry of planar imidazole. Consequently, our theoretical findings indicate the reaction mechanisms for path III-1 and path III-2 should proceed as follows:

$$\text{Path III-1: } \mathbf{1}(S_0) + h\nu \rightarrow \mathbf{FC-1} \rightarrow \mathbf{CI-III-1} \rightarrow \mathbf{2} \quad (5)$$

$$\text{Path III-1: } \mathbf{1}(S_0) + h\nu \rightarrow \mathbf{FC-1} \rightarrow \mathbf{CI-III-2} \rightarrow \mathbf{3} \quad (6)$$

Our MP2-CAS results shown in Figure 6 indicate that **CI−III-1** is 61 kcal/mol lower in energy than **FC−1**, whereas **CI−III-2** lies 41 kcal/mol below **FC−1**. Competition between these reaction paths is presumably governed by the relative energies of the CIs involved.[13] As a result, path III-1 would be more favorable than path III-2 from an energetic viewpoint,

suggesting that the quantum yield of 1,2,4-trimethylimidazole (**2**) should be larger than that of 1,2,5-trimethylimidazole (**3**). These theoretical findings are in agreement with the experimental observation of the formation of **2** and **3**, the former being the major phototransposition product.

Briefly, our model investigations demonstrate that upon absorption of a photon of light, 1,3,5-trimethylpyrazole (**1**) is excited vertically to S_1 followed by a rapid relaxation, via a CI, to its ground-state surface, where it undergoes a radiationless transition from **1** to photoproduct imidazoles (i.e., **2** and **3**).

V. Conclusion

The photochemical reaction pathways of 1,3,5-trimethylpyrazole (**1**) were investigated by ab initio calculations at the CAS(8,6)/6-311G(d) and MP2-CAS-(8,6)/6-311G(d) levels of theory. In the present work, three reaction pathways, the ring-contraction−ring-expansion route (paths I-1 and I-2), the internal-cyclization−isomerization route (paths II-1 and II-2), and the CI route (paths III-1 and III-2), were examined theoretically. By taking all the mechanisms studied in this paper together, one can obtain the following conclusions.

(1) From this study, we can elaborate on the standard model of the photochemistry of 1,3,5-trimethylpyrazole (**1**). It is found that a knowledge of the CIs of pyrazole species is of great importance in understanding their reaction mechanisms, because it can affect the driving force for photochemistry. For instance, 1,3,5-trimethylpyrazole (**1**) is vertically excited to the S_1 state. Then, radiationless decay from S_1 to S_0 of **1** occurs via a CI, which results in a rapid ring bond rotation. By starting from this CI, the products of the phototranpositions as well as the initial reactant can be reached on a barrier-less ground-state relaxation path.[6] As a result, these findings, based on the CI viewpoint, have helped us better understand the photochemical reactions and support the experimental observations.[2−5]

(2) It has been generally assumed in the past that the photoisomerization of **1** could follow either the ring-contraction−ring-expansion or the internal-cyclization−isomerization sequence. The former mechanism (paths I-1 and I-2) appears to occur via ring contraction to form a three-membered ring analogue. This then undergoes ring expansion to give the rearranged five-membered ring product. Alternatively, the latter mechanism (paths II-1 and II-2) involves an initial disrotatory formation of a bicyclic isomer, followed by a [1,3] sigmatropic shift to a second bicyclic isomer. This then undergoes a disrotatory ring opening to yield the rearranged product. In addition, we suggested a third mechanism, the CI mechanism (paths III-1 and III-2) to rationalize the photorearrangements of 1,3,5-trimethylpyrazole (**1**). However, our model investigations indicate that both the ring-contraction−ring expansion and the internal-cyclization−isomerization mechanisms involve several high-energy transition structures, which makes them energetically unfeasible from a kinetic viewpoint. Moreover, it should be noted that the third mechanism (the CI route) is a one-step process, whereas the other two mechanisms are multistep processes. As a result, we predict that the CI mechanism should be favored over the ring-contraction−ring expansion and the internal-cyclization−isomerization mechanisms from a kinetic viewpoint.

(3) In the third mechanism (the CI route), our computational results also indicate that **CI−III-1** is lower in energy than **CI−III-2** by 20 kcal/mol. The theoretical findings thus predict that path III-1 should be favored over path III-2 from a kinetic point of view. Indeed, it was reported that **1** undergoes photoisomerization to give ca. 26% **2** and only 10% photoproduct **3**.[3] Consequently, our theoretical predictions presented in this work are in good agreement with the experimental observations.

(4) In the present work, we propose a simple p-π orbital topology model, which can be used as a guide to predict the location at which CIs are likely to occur, as well as the conformations of the phototransposition products of various heterocycles. The results presented here, together with our work on the photochemistry of other 5- and 6-membered heterocycles,[13] appear to give convincing evidence that CIs play a crucial role in such photoisomerizations and that they are directly involved in heterocycle photochemistry and photophysics.

Acknowledgment. The author is grateful to the National Center for High-Performance Computing of Taiwan for generous amounts of computing time, and the National Science Council of Taiwan for the financial support. The author also wishes to thank Professor Michael A. Robb, Dr. Michael J. Bearpark, (University of London, UK) and Professor Massimo Olivucci (Universita degli Studi di Siena, Italy) for their encouragement and support. Special thanks are also due to reviewers 1, 2, and 3 for very helpful suggestions and comments.

References and Notes

(1) For reviews, see: (a) De. Mayo, P. In *Rearrangements in Ground and Excited States*; Academic Press: New York, 1980, Vol. *3*. b) Buchardt, O. In *Photochemistry of Heterocyclic Compounds*; Wiley: New York, 1976. (c) Kopecky, J. In *Organic Photochemistry: A Visual Approach*; VCH Publishers: New York, 1992.

(2) Padwa, A. In *Rearrangements in Ground and Excited States*; de Mayo, P., Ed.; Academic Press: New York, 1980; Vol. 3, p 529 ff.

(3) (a) Tiefenthaler, H.; Dorscheln, W.; Goth, H.; Schmid, H. *Tetrahedron Lett.* **1964**, 2999. (b) Goth, H.; Tiefenthaler, H.; Dorschlen, W. *Chimia* **1965**, *19*, 596. (c) Ferris, J. P.; Orgel, L. E. *J. Am. Chem. Soc.* **1966**, *88*, 1974. (d) Gaaneux, A. R.; Goschke, R. *Tetrahedron Lett.* **1966**, 5451. (e) Beak, P.; Miesel, J. L.; Messer, W. R. *Tetrahedron Lett.* **1967**, 5315. (f) Tiefenthaler, H.; Dorscheln, W.; Goth, H.; Schmid, H. *Helv. Chim. Acta* **1967**, *50*, 2244. (g) Ege, S. N. *Chem. Commun.* **1967**, 488. (h) Reisch, J.; Fitzek, A. *Tetrahedron Lett.* **1967**, 4513. (i) Ege, S. N. *J. Chem. C* **1969**, 2624. (j) Reisch, J.; Fitzek, A. *Tetrahedron Lett.* **1969**, 271. (k) Beak, P.; Messer, W. *Tetrahedron.* **1969**, *25*, 3287.

(4) Pavlik, J. W.; Kebede, N. *J. Org. Chem.* **1997**, *62*, 8325.

(5) (a) Barltrop, J. A.; Day, A. C.; Mack, A. G.; Shahrisa, A.; Wakamatsu, S. *Chem. Commun.* **1981**, 604. (b) Pavlik, J. W.; Kurzweil, E. M. *J. Org. Chem.* **1991**, *56*, 6313. (c) Connors, R. E.; Pavlik, J. W.; Burns, D. S.; Kurzweil, E. M. *J. Org. Chem.* **1991**, *56*, 6321. (d) Connors, R. E.; Burns, D. S.; Kurzweil, E. M.; Pavlik, J. W. *J. Org. Chem.* **1992**, *57*, 1937. (e) Pavlik, J. W.; Connors, R. E.; Burns, D. S.; Kurzweil, E. M. *J. Am. Chem. Soc.* **1993**, *115*, 7645. (f) Pavlik, J. W.; Kebede, N.; Bird, N. P.; Day, A. C.; Barltrop, J. A. *J. Org. Chem.* **1995**, *60*, 8138.

(6) For recent, excellent reviews, see: (a) Bernardi, F.; Olivucci, M.; Robb, M. A *Isr. J. Chem.* **1993**, 265. (b) Klessinger, M. *Angew. Chem., Int. Ed. Engl.* **1995**, *34*, 549. (c) Bernardi, F.; Olivucci, M.; Robb, M. A. *Chem. Soc. Rev.* **1996**, 321. (d) Bernardi, F.; Olivucci, M.; Robb, M. A. *J. Photochem. Photobiol. A* **1997**, *105*, 365. (e) Klessinger, M. *Pure Appl. Chem.* **1997**, *69*, 773. (f) Klessinger, M.; Michl, J. In *Excited States and Photochemistry of Organic Molecules*; VCH Publishers: New York, 1995.

(7) (a) Olivucci, M.; Ragazos, I. N.; Bernardi, F.; Robb, M. A. *J. Am. Chem. Soc.* **1993**, *115*, 3710. (b) Bernardi, F.; Olivucci, M.; Ragazos, I. N.; Robb, M. A. *J. Am. Chem. Soc.* **1992**, *114*, 8211.

(8) Frisch, M. J.; Trucks, G. W.; Schlegel, H. B.; Scuseria, G. E.; Robb, M. A.; Cheeseman, J. R.; Montgomery, J. A., Jr.; Vreven, T.; Kudin, K. N.; Burant, J. C.; Millam, J. M.; Iyengar, S. S.; Tomasi, J.; Barone, V.; Mennucci, B.; Cossi, M.; Scalmani, G.; Rega, N.; Petersson, G. A.; Nakatsuji, H.; Hada, M.; Ehara, M.; Toyota, K.; Fukuda, R.; Hasegawa, J.; Ishida, M.; Nakajima, T.; Honda, Y.; Kitao, O.; Nakai, H.; Klene, M.; Li, X.; Knox, J. E.; Hratchian, H. P.; Cross, J. B.; Bakken, V.; Adamo, C.; Jaramillo, J.; Gomperts, R.; Stratmann, R. E.; Yazyev, O.; Austin, A. J.; Cammi, R.; Pomelli, C.; Ochterski, J. W.; Ayala, P. Y.; Morokuma, K.; Voth, G. A.; Salvador, P.; Dannenberg, J. J.; Zakrzewski, V. G.; Dapprich, S.; Daniels, A. D.; Strain, M. C.; Farkas, O.; Malick, D. K.; Rabuck, A. D.; Raghavachari, K.; Foresman, J. B.; Ortiz, J. V.; Cui, Q.; Baboul, A. G.; Clifford, S.; Cioslowski, J.; Stefanov, B. B.; Liu, G.; Liashenko, A.; Piskorz, P.; Komaromi, I.; Martin, R. L.; Fox, D. J.; Keith, T.; Al-Laham, M. A.; Peng, C. Y.; Nanayakkara, A.; Challacombe, M.; Gill, P. M. W.; Johnson, B.; Chen, W.; Wong, M. W.;

Gonzalez, C.; Pople, J. A. *Gaussian 03*, revision C.02; Gaussian, Inc.: Wallingford, CT, 2004. (b) Bearpark, M. J.; Robb, M. A.; Schlegel, H. B. *Chem. Phys. Lett.* **1994**, *223*, 269.

(9) McDouall, J. J. W.; Peasley, K.; Robb, M. A. *Chem. Phys. Lett.* **1988**, *148*, 183.

(10) Swaminathan, M.; Dorgra, S. K. *Indian J. Chem.* **1983**, *22A* 853.

(11) The C−C, C−N, C−H, N−CH_3, and C−CH_3 bonds in **1** are fixed to be 1.44, 1.35, 1.09, and 1.45 Å, respectively. Also, ∠NCC, ∠CNC, ∠NCN, ∠NCH, ∠HCH, and ∠CCC bond angles are fixed to be 106, 106, 110, 120, 109, and 120°, respectively.

(12) One vetor leads to the final photoproduct, whereas the other vector may lead to a vibrationally hot S_0 species.

(13) (a) Su, M.-D *J. Phys. Chem. A.* **2006**, *110*, 9420. (b) Su, M.-D *J. Phys. Chem. A* **2006**, *110*, 12653. (c) Su, M.-D *J. Phys. Chem. A* **2008**, *112*, 5527. (d) Su, M.-D. *J. Chem. Theory Comput.* **2008**, ASAP.

JP805394K